ACTA STEREOL 1995; 14/1: 35-44
STERMAT'94
ORIGINAL SCIENTIFIC PAPER

ROUGHNESS INVESTIGATION BY MATHEMATICAL MORPHOLOGY

Michel COSTER, Gervais GAUTHIER, Jean-Louis CHERMANT

Laboratoire d'Etudes et de Recherches sur les Matériaux,
LERMAT, URA CNRS n° 1317, ISMRA-Université
6 Bd du Maréchal Juin , 14050 CAEN Cedex, France

ABSTRACT

Several methods can be used to characterize the roughness of non planar surfaces. These surfaces, in the case of non overlapping can be represented by $\mathbb{R}^2 * \mathbb{R}$ functions. In this paper we present the methods derived from mathematical morphology for functions which can be used to analyse these surfaces. $\mathbb{R}^2 * \mathbb{R}$ functions can be obtained from true relief or perspective image. These two cases are discussed in terms of anamorphosis. The basic parameters are briefly introduced. Different morphological functions (granulometry, roughness, connectivity number), are presented and discussed after tests on real or simulated images.

Key words : non planar surfaces, roughness, mathematical morphology, granulometry.

INTRODUCTION

The characterization of non planar surfaces is very important in many fields of application as fractography, roughness studies on metallic sheets, skin studies and so on. The choice of the method of characterization depends on several prerequisites. The first of all is the nature of the relief. If the non planar surfaces have overlapping parts, the relief can be described in $\mathbb{R}^3$ space and we must use, for example, 3D mathematical morphology. But, if no overlapping exists the relief can be described by $\mathbb{R}^2 * \mathbb{R}$ functions. In this case, the corresponding grey tone image is the subgraph of the function and its surface is the graph. In these conditions mathematical morphology and stereology for functions can be used. When overlapping exists on the non planar surface, only *profilometric analysis* can be used. This kind of surface appears mainly for ductile fractures. In this paper, we shall consider only the more general case of non overlapping and, after a brief recall on stereological measurements for functions, some general methods will be proposed to describe non planar surfaces by mathematical morphology.

THE DIFFERENT IMAGE ACQUISITIONS

From non planar surfaces without overlapping, the grey tone images can be obtained by two main ways. If the relief is studied by using a 3D roughness apparatus or a confocal microscope, the grey tone image corresponds to the *true relief*. The grey level gives the altitude of each point.
If the image is obtained via a scanning electron microscope (SEM), one obtains a *perspective image* where the value of each pixel does not correspond to the altitude. However, an unknown relation exists given by the *transfer function* of the apparatus. In the case of SEM images, a very simplified transfer function has been proposed by Hénault et *al.* (1994) which conserves the classification of roughness.

When overlapping exists, the fracture surface must be cut by an approximately perpendicular plane and the obtained profile can be observed and analysed with SEM or optical microscope.

PARAMETRIC ANALYSIS OF $\mathbb{R}^2_*\mathbb{R}$ FUNCTIONS

In previous papers (Coster, 1992; Hénault and Chermant, 1992), the basic parameters for $\mathbb{R}^2_*\mathbb{R}$ functions derived from classical stereological parameters have been described. According to the set meaning, a $\mathbb{R}^2_*\mathbb{R}$ function **f** is mainly characterized by its support **Z** and its area A(**Z**), by the *surface* S(**f**) of its *graph* G(**f**), and by the *volume* V(**f**) of its *subgraph* SG(**f**). The topological property of the function is given by the *integral of connectivity* N_2(**f**) which corresponds to the sum of the local maxima heights minus the sum of local minima heights. Table 1 presents these parameters given in the local case.

Table 1. Local parameters for $\mathbb{R}^2_*\mathbb{R}$ functions : Π_t represents an horizontal plane at level t; the intersection is given by the threshold at level t.

Local parameter	Definition	Meaning
Volume per unit area of support	$V_A(\mathbf{f}) = \frac{V(SG(\mathbf{f}))}{A(\mathbf{Z})}$	Mean value of the function
Surface area per unit area of support	$S_A(\mathbf{f}) = \frac{S(G(\mathbf{f}))}{A(\mathbf{Z})}$	equivalent to surface roughness $R_A(\delta\mathbf{X})$
Integral connectivity number per unit area of support	$N_A(\mathbf{f}) = \frac{\int N_2(SG(\mathbf{f}) \cap \Pi_t)\, dt}{A(\mathbf{Z})}$	equivalent to vertical roughness for surfaces

These stereological parameters for $\mathbb{R}^2_*\mathbb{R}$ functions can be used without problem on true relief, but their values are function of anamorphosis in other cases. V_A(**f**) is only used for morphological functions like granulometry. The two last parameters can be used directly on function or for morphological function.

CHARACTERISATION OF SURFACE BY GRANULOMETRIC FUNCTIONS

Mathematical morphology for functions

In mathematical morphology for functions, the tools can be classified in two main classes (Chermant and Coster, 1994). The first one corresponds to *filtering process*. In this case, the morphological transformation are the basic filters (opening and closing) and complex filters like sequential filters and autodual filters. The second class is used for the *segmentation process*. In this case, the watershed is the most useful tool.

For the functions, two kinds of structuring elements can be used, *volumic structuring elements* (Fig. 1b,1c,1d) and *flat structuring element* (Fig. 1a). In the case of $\mathbb{R}^2_*\mathbb{R}$ functions, the volumic structuring element has the same mixed (i.e. non homogeneous) dimension as the image. For flat structuring element, the modulus of the third dimension, corresponding to the grey level, is zero. This is the reason why these structuring elements do not change with *anamorphosis*.

When a morphological filtering is used, the « absolute result » is different between original image and anamorphosed image with any structuring element. But the « relative result » is the same when flat structuring element is used. So, the ratio between basic measurements performed on the transformed image and a reference (initial) image is always the same and is

independent on anamorphosis. Of course, this property is not satisfied using a volumic element.

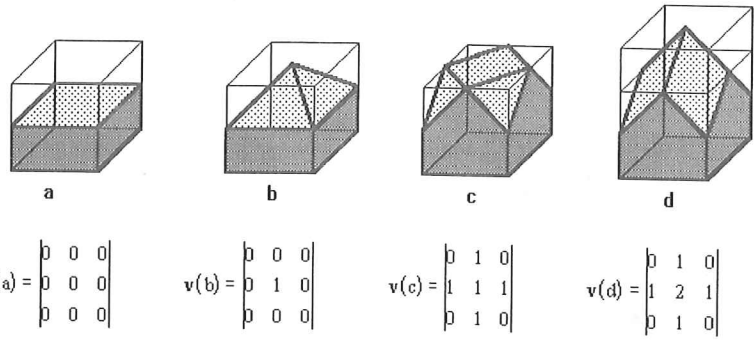

Fig. 1. Main structuring elements for $\mathbb{R}^2_*\mathbb{R}$ functions with support digitised on a square lattice and their neighbourhood function $\mathbf{v}(i)$: flat structuring element (a), volumic structuring elements (b = pyramid, c = cuboctaedron, d = rhombododecaedron).

Surface roughness and granulometry

The granulometric methods are very well adapted to describe non planar surfaces. Moreover the granulometry is the first morphological method used (Michelland et *al*, 1989; Prod'homme et *al.* 1992). *Granulometric transformation* (Serra, 1988) is a class of basic morphological filtering (*opening* or *closing*) when the structuring element is convex and depends on size criterion λ. The variation of λ gives a family of similar structuring elements. The *granulometric distribution* is then given by :

$$G(\mathbf{f}_{\lambda B}) = \frac{V(\mathbf{f}) - V(\gamma^{\lambda B}\mathbf{f})}{V(\mathbf{f})} \qquad (1)$$

where $\gamma^{\lambda B}\mathbf{f}$ is the morphological opening of the function by the convex structuring element B of size λ. With closing $\varphi^{\lambda B}\mathbf{f}$, one obtains an *antigranulometric distribution* given by :

$$G(\mathbf{f}^{\lambda B}) = \frac{V(\varphi^{\lambda B}\mathbf{f}) - V(\mathbf{f})}{V(\mathbf{f})} \qquad (2)$$

When the structuring element is flat the granulometric distribution is independent on increasing anamorphosis. This is very important in the case of SEM images where the signal is always anamorphosed. These two cumulative distributions can be derived to obtain the corresponding histograms $g(\mathbf{f}_{\lambda B})$ and $g(\mathbf{f}^{\lambda B})$.

Critical studies of granulometries on non planar surfaces

To analyse the behavior of granulometric transformations on a relief or SEM image of non planar surfaces, several kinds of image were used : simulated relief and fracture surface observed by SEM. The first class of simulated images is obtain by using boolean functions (Fig.3), whereas the second class (Fig.4) is built from fractal algorithm (Barnsley et *al*, 1988). The SEM images used are obtained from brittle fracture of alumina (Fig.4) or ductile fracture of steel (Fig.5). In all cases the granulometries were performed with the flat structuring element to avoid the bias introduced by anamorphosis.

Contrary to linear filters, the opening and the closing processes are not symmetrical filter since opening removes narrow peaks and crests whereas closing fills narrow valleys and basins. The choice of the opening or closing to perform granulometries on a relief depends on its nature.

In the case of boolean surface where the convex grains define the relief, the opening is the right choice. The principal mode of the distribution (Fig. 6 curve γ) corresponds to the size of the mean primary grain, whereas the secondary mode obtained for the great values of λ corresponds to the clusters of primary grains. For the closing distribution, the mode corresponds to the mean size of the valleys (Fig. 6, curve ϕ).

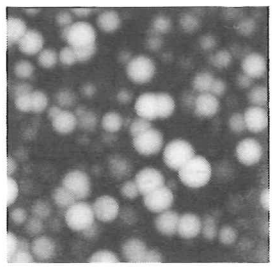

Fig. 2. Simulation of a boolean surface.

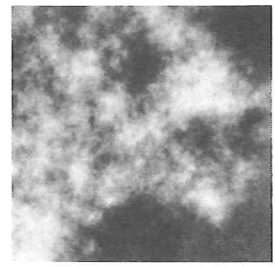

Fig. 3. Simulation of a fractal surface.

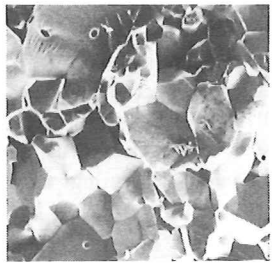

Fig. 4. Brittle fracture of alumina.

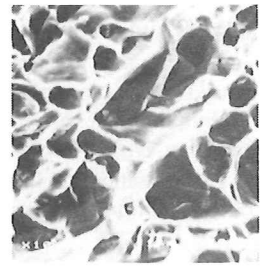

Fig. 5. Ductile fracture of steel.

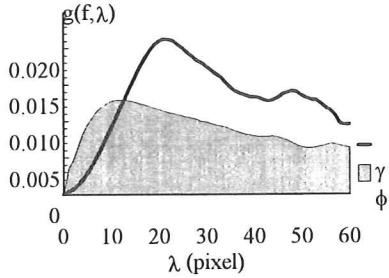

Fig. 6. Granulometric densities g(**f**) by opening (γ) and closing (ϕ) for a booleean function.

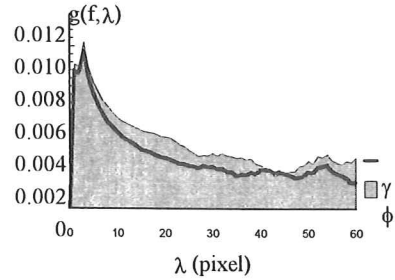

Fig. 7. Granulometric densities g(**f**) by opening (γ) and closing (ϕ) for a fractal image (D=2.5).

For fractal images, (Fig. 7), the mode of the distribution by opening and closing, obtained for the small values of λ, corresponds to a problem between the algorithm defined in the continuous space and its application in digital space. After some steps the distribution is approximately flat and corresponds to the auto-similarity of the image. This behavior is the same for all the fractal dimensions tested.

In the case of alumina, the crests and the valleys are approximately symmetric. This is the reason why the distributions by opening or closing are similar, except for the low values of λ (Fig. 8).
Finally with the ductile fracture of steels, the result is not symmetrical for opening and closing. The mode of the distribution by closing corresponds to the mean size of the dimples (Fig. 9, curve γ), whereas the mode of distribution by opening corresponds to the mean size of the crests between dimples, (Fig. 9, curve ϕ).

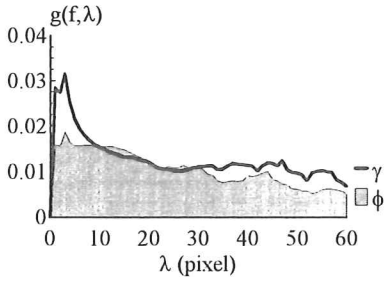

Fig. 8. Granulometric densities g(**f**) by opening (γ) and closing (ϕ) for brittle fracture surface of alumina.

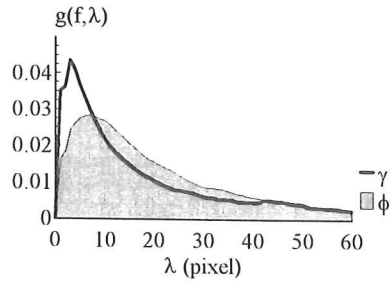

Fig. 9. Granulometric densities g(**f**) by opening (γ) and closing (ϕ) for ductile fracture surface of steel.

CHARACTERIZATION BY SURFACE ROUGHNESS FUNCTION

Definition of surface roughness function

Roughly speaking, the *roughness function* is defined by the evolution of the surface area of the graph as a function of the size of the gauge used to perform measurements. In the local case, the surface area is replaced by the surface roughness parameter $S_A(\mathbf{f})$ defined in table 1. To obtain an estimation of the surface area several methods are possible, but the only one which depends on a gauge is the Steiner method defined by the following relation :

$$S(\mathbf{f}) = \lim_{\lambda \to 0} \frac{V\left(\delta^{\lambda B}\mathbf{f}\right) - V\left(\varepsilon^{\lambda B}\mathbf{f}\right)}{2\lambda} \tag{3}$$

where $\delta^{\lambda B}\mathbf{f}$ is the dilated function by the structuring element λB and $\varepsilon^{\lambda B}\mathbf{f}$ the corresponding eroded function. Then, the surface roughness is obtained by the equation given in table 1. If λ does not tend towards zero, one obtains an approximate surface roughness function of λ defined by equation (4) :

$$S(\mathbf{f},\lambda) = \frac{V\left(\delta^{\lambda B}\mathbf{f}\right) - V\left(\varepsilon^{\lambda B}\mathbf{f}\right)}{2\lambda} \tag{4}$$

This approach is very similar to the methods used by several authors in profilometric analysis to estimate a fractal dimension (Chermant and Coster, 1983; Chermant et *al.* 1983), but different from the fractal methods proposed by Underwood and Banerji (1986) or Baran et *al.* (1992). The absolute surface roughness function, defined by equation (5) :

$$S_A(\mathbf{f},\lambda) = \frac{S(\mathbf{f},\lambda)}{A(\mathbf{Z})} \tag{5}$$

depends on anamorphosis for all classes of structuring elements. This is not important for the true reliefs, but very important for perspective images obtained with a SEM. This is the reason why we have proposed (Gauthier et *al*, 1994) another parameter called the *relative roughness* and defined by equation (6) :

$$R_S(\mathbf{f},\lambda) = \frac{S(\mathbf{f},\lambda)}{S(\mathbf{f},\lambda_0)} \tag{6}$$

where λ is the current step of measurement and λ_0 is the shortest step (size of one pixel).
The division of the surface area $S(\mathbf{f}, \lambda)$ by the surface area $S(\mathbf{f}, \lambda_0)$ reduces the influence of the anamorphosis. Only the transformation depends on it, like for the granulometries. If the flat structuring element is employed then the measurement is independent on the anamorphosis (Fig. 11). It is not the case for volumic structuring elements (Fig. 10).

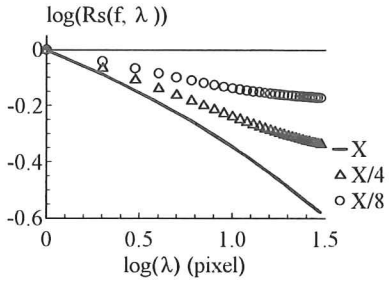

Fig. 10. Effect of anamorphosis on $R_S(\mathbf{f})$ function by dividing the scale of grey levels (SEM image of alumina and rhombododecaedron element).

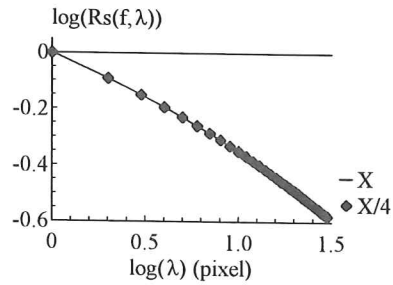

Fig. 11. Effect of anamorphosis on $R_S(\mathbf{f})$ function by dividing the scale of grey levels (SEM image of alumina and flat element).

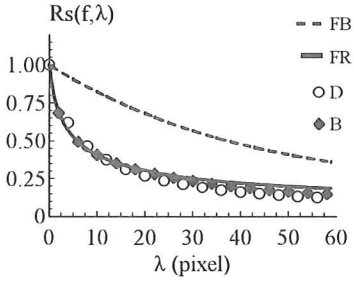

Fig. 12. Relative roughness $R_S(\mathbf{f},\lambda)$ for boolean function (FB), fractal surface (FR), brittle fracture surface of alumina (B) and ductile fracture surface of steel (D) with flat structuring element.

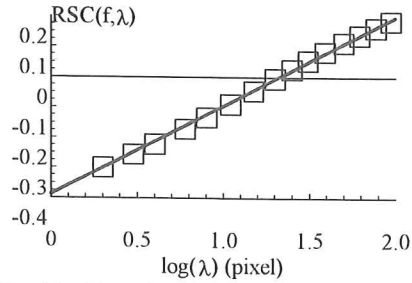

Fig. 13. Linearized RSCs as a function of relative roughness $R_S(\mathbf{f},\lambda)$ for ductile fracture surface of steel versus the size of cuboctaedron element.

Fig. 12 exhibits the relative roughness function for the four types of tested images with flat structuring element. The shape of the $R_S(\mathbf{f},\lambda)$ is approximately the same for all the images, but the values of this function in the case of fracture surfaces observed by SEM are closer to fractal surface than boolean surface. This fact is often interpreted in terms of fractal model for

fracture surfaces. The curves in figures 10 and 11, drawn according to a fractal plot, are not linear and so cannot be described by an ideally fractal model. Underwood and Banerji (1986) have proposed a derived model (RSC) where the fractal plot is sigmoidal to describe this evolution. The expression of the *reverse sigmoid function* for $R_S(\mathbf{f},\lambda)$ is given by the following equation 7 :

$$RSC(R_s,\lambda) = \log\left\{\log\left[\frac{R_s(\mathbf{f},0)-1}{R_s(\mathbf{f},\lambda)-1}\right]\right\} = b + m\log(\lambda) \qquad (7)$$

Figure 13 is obtained by the linearization of reversed fractal curve (RSC) for ductile fracture of steel with volumic structuring element. The experimental points fit very well with a linear variation according to equation 7. However the fit is better for the fractal image. To see the influence of the structuring element on the results of the fractal plot, we have computed $R_S(\mathbf{f},\lambda)$ as function of λ on the same classes of images, (Fig. 14 and 15).

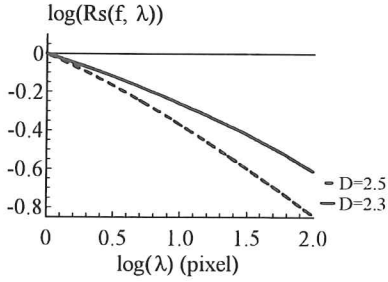

Fig. 14. Relative roughness $R_S(\mathbf{f},\lambda)$ for fractal surfaces with flat structuring element.

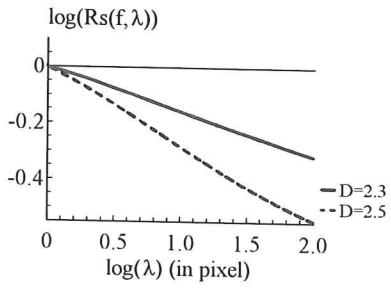

Fig. 15. Relative roughness $R_S(\mathbf{f},\lambda)$ for fractal surfaces with cuboctahedron structuring element.

In all the cases the slope of the curve increases with the simulated dimension. But, in the case of flat structuring element (Fig 14), the curves do not correspond to a straight line, whereas in the case of volumic cuboctahedron element the curves can be fitted by a linear plot, (Fig 15). To see the influence of the shape of the structuring elements defined in Fig. 1, those have been used on simulated fractal surfaces. The curves are drawn on Fig. 16 and 17. The statistical data of the linear regression are presented in table 2. Some comments can be written about these results :

- the cubic and cuboctahedron elements give the best linear regression and the lowest residual variation, the rhombododecahedron gives the most bad result,
- the slopes obtained with pyramid, cuboctahedron and cubic element belong to the same range of values,
- for the flat structuring element the slope is approximately twice the value of the previous volumic structuring elements and the slope corresponding to rhombododecahedron is approximately half the slope of the other volumic elements.

This last comment can be explained by the upper value of the neighbouring function given in Fig. 1. The slope decreases when the « roughness » of the structuring element increases in the same proportion. If the theoretical value of the fractal simulation is compared with the slopes, the flat structuring element seems to give the best results. But when the size of the structuring element tends to infinity, it is easy to proof that the slope must reach asymptotically the value (-1) for all non planar surfaces. In the case of volumic elements, any asymptotical behavior can be obtained independently on the nature of the surface.

Table 2. Statistical values of linear regression for $\text{Log}(R_S(\mathbf{f},\lambda)) = f(\text{Log}(\lambda))$ for fractal surface of theoretical fractal dimension 2.3, by using the Steiner method with various structuring elements.

(100 pts tested)	Flat	Pyramidal	Cubocta-hedron	Cubic	Rhombodo-decahedron
origin	0.0632	-0.0170	0.0013	0.0010	-0.0342
slope	-0.3298	-0.1815	-0.1585	-01699	-0.0864
correlation	-0.9960	-0.9968	-0.9999	-0.9997	-0.9800
residual value	0.0012	0.0058	0.0008	0.0005	0.0071

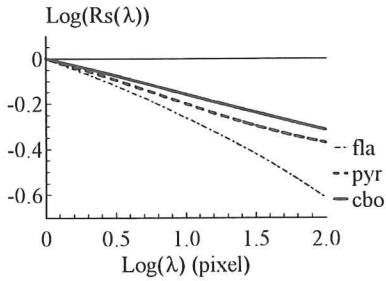

Fig. 16. Relative roughness $R_S(\mathbf{f},\lambda)$ for a fractal surface with flat, pyramidal and cuboctahedron structuring element.

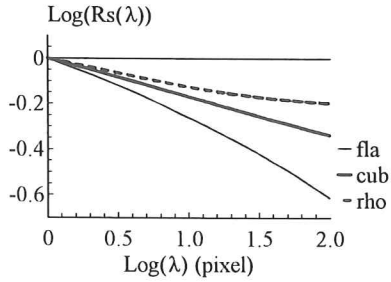

Fig. 17. Relative roughness $R_S(\mathbf{f},\lambda)$ for a fractal surface with flat, cubic and rhombododecahedron structuring element.

FUNCTION CHARACTERIZATION BY CONNECTIVITY NUMBER

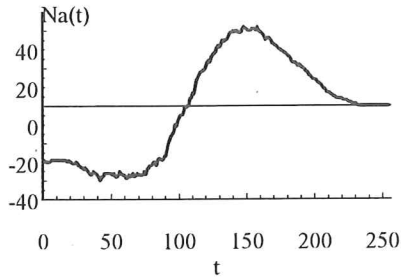

Fig. 18. Connectivity number function $N_A(t)$ for a boolean surface per frame unit.

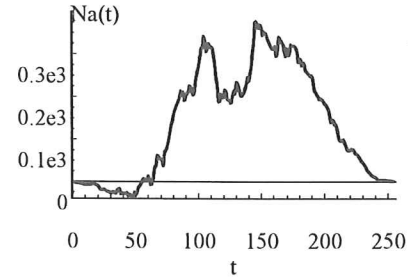

Fig. 19. Connectivity number function $N_A(t)$ for a fractal surface per frame unit.

The last local parameter $N_A(\mathbf{f})$, called most commonly « *vertical roughness for surfaces* » is too general to describe correctly the peaks and basins for non planar surfaces. To describe more accurately these morphological features, it is possible to measure the *specific connectivity number* $N_A(SG(\mathbf{f})\cap\Pi_t)$ at each level t and draw its evolution. So one defines the *connectivity number function* for a surface $N_A(t) = N_A(SG(\mathbf{f})\cap\Pi_t)$ as a function of t. Figures 18 to 21 represent this new functional for the four types of analysed surfaces.

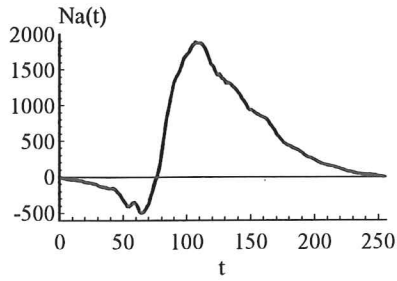

Fig. 20. Connectivity number function $N_A(t)$ for a brittle fracture surface per frame unit.

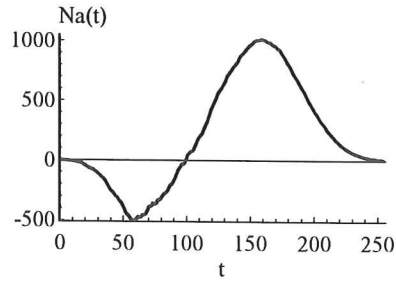

Fig. 21. Connectivity number function $N_A(t)$ for ductile fracture surface per frame unit.

To understand the evolution of $N_A(t)$, one must imagine that the relief is progressively immersed in the sea. For each step of immersion, the connectivity number gives the number of continents or islands minus the number of lakes or closed seas.
The chosen conditions for the construction of this boolean surface gives a function which covers only 95% of the area of the support. This is the reason why the connectivity number function starts from a negative value corresponding to residual lakes. For the other models, one starts from a relief without water ($N_A(0) = 0$). Afterwards, progressively the deep basin are filled by water. With these conditions the first values of $N_A(t)$ are negative. When the immersion progresses, some islands are isolated from the continent and the value of $N_A(t)$ increases toward positive domain. This increasing stops when all mountains are isolated to give islands. The final behavior corresponds to a decrease of the connectivity number when the lowest islands are immersed. To resume, the minimum of the function corresponds to the maximum number of basins and its position on t axis gives the altitude. The maximum of the function corresponds to the maximum of peaks and its position corresponds to the altitude.
For each class of surface, the behavior is not the same : the evolution for boolean surface is the most symmetric in opposition to fractal surface where one observes few number of little basins and a great number of peaks. For fracture surfaces the ductile behavior gives a great number of basins (dimples), whereas the basins correspond to triple boundaries of grains in intergranular fracture.
Since the measurements are performed on threshold image at level t, the effect of the anamorphosis is very well known. An anamorphosis of the image implies the same anamorphosis of t axis. So the result is independent on anamorphosis if relative t values are used.

CONCLUSION AND PERSPECTIVES

Mathematical morphology is very well adapted to study non planar surfaces by the image of true relief or by perspective image. In this paper, only non overlapping surfaces were analysed and discussed.
For this class of surface, the three basic function derived from the three corresponding parameters were presented : granulometric functions, relative roughness function and connectivity number function.
The granulometric function is well adapted to describe the size of the texture of the surface and is independent on anamorphosis when flat structuring element is used.
To avoid the effect of anamorphosis the relative roughness parameter must be used in place of absolute surface roughness. Since the surface morphology can be analysed in term of fractal

model, the influence of the anamorphosis and of the nature of the structuring element were analysed and discussed. To be independent on anamorphosis, flat structuring elements must be used, but with these elements, it is theoretically impossible to estimate a fractal dimension. Indeed, in fractal analysis, the ball which is used to test a fractal object by a covering method must have a topological dimension equals to the dimension of the object plus one. This is the main problem in fractal analysis when anamorphosis occurs. In the case of volumic element, fractal analysis can be performed, but as for in granulometry or other morphological transformations the result depends on the shape of the used structuring element.

The connectivity number function gives other knowledge on the morphology of the surface than roughness and granulometry since it is possible to see the influence of basins and peaks without problem of anamorphosis.

These methods described for $\mathbb{R}^2 * \mathbb{R}$ functions can be used directly in profilometric analysis on non overlapping profiles or on $\mathbb{R}^1 * \mathbb{R}$ functions. When overlapping exists, granulometric analysis with flat structuring element (segment) can be used without restriction. The roughness or relative roughness function can be obtained by using bidimensional structuring element. Finally the connectivity number function is given by the measure of the horizontal intercepts.

REFERENCES

Baran GR, Rocques-Carmes C, Wehbi D, Degrange M. Fractal characteristics of fracture surfaces. J Am Ceram Soc 1992; **75**: 2687-2691.

Barnsley MF, Devaney RL, Mandelbrot BB, Peitgen HO, Saupe D, Voss RF. in The Science of Fractal Images. Berlin : Springer-Verlag 1988; p 95-105.

Chermant JL, Coster M. Survey of quantitative fractography in materials sciences. Acta Stereol 1983; **2/1**: 55-64.

Chermant L, Chermant JL, Coster M. Simulation of brittle fracture profile. Acta Stereol 1983; **2/1**: 71-74.

Chermant JL, Coster M. Role of mathematical morphology in filtering, segmentation and analysis. 6ECS, Praha, Sept. 7-10, 1993. Acta Stereol 1994; **13/2**: 125-136.

Coster M. Tools for non planar surfaces. Acta Stereol 1992; **11/1**: 639-650.

Gauthier G, Rebillon JO, Coster M, Hénault E. Grey tone level images characterization by morphological functions : application to non planar surfaces. 6ECS, Praha, Sept. 7-10, 1993. Acta Stereol 1994; **13/2**: 155-160.

Hénault E, Chermant JL. Parametrical investigation of grey tone image. Acta Stereol 1992; **11/1**: 665-670.

Hénault E, Chermant JL, Coster M. Simulation of the observed image of a relief : notion of transfer function. 6ECS, Praha, Sept. 7-10, 1993. Acta Stereol 1994; **13/2**: 161-167.

Michelland S, Schiborr B, Coster M, Mordike BL, Chermant JL. Size distribution of granular materials from unthreshold image. J Microscopy 1989; **156**: 303-311.

Prod'homme M, Chermant L, Coster M. Texture analysis of ceramic films by image processing. J Microscopy 1992; **168**: 15-23.

Serra J. Image Analysis and Mathematical Morphology. Vol 2 : Theoretical Advances. Academic Press, 1988.

Underwood EE., Banerji K. Fractals in fractography. Mat Sci Eng 1986; **80**: 1-14.